

Characteristics of Eu^{2+} , Dy^{3+} -Doped SrAl_2O_4 Synthesized by Hydrothermal Reaction and Its Photocatalytic Properties

Byung-Geon Park

Department of Food and Nutrition, Kwangju Women's University, Gwangju, Republic of Korea
Email: bgpark@kwu.ac.kr

How to cite this paper: Park, B.-G. (2018) Characteristics of Eu^{2+} , Dy^{3+} -Doped SrAl_2O_4 Synthesized by Hydrothermal Reaction and Its Photocatalytic Properties. *Journal of Materials Science and Chemical Engineering*, 6, 12-21.

<https://doi.org/10.4236/msce.2018.62002>

Received: December 29, 2017

Accepted: February 9, 2018

Published: February 12, 2018

Copyright © 2018 by author and Scientific Research Publishing Inc.

This work is licensed under the Creative Commons Attribution International License (CC BY 4.0).

<http://creativecommons.org/licenses/by/4.0/>



Open Access

Abstract

Eu^{2+} , Dy^{3+} -doped SrAl_2O_4 was prepared by a hydrothermal reaction through the process of calcination at lower temperature. The physicochemical properties of the SrAl_2O_4 : Eu^{2+} , Dy^{3+} phosphor were characterized and compared to those of the SrAl_2O_4 : Eu^{2+} , Dy^{3+} prepared by sol-gel method. The photocatalytic properties of the SrAl_2O_4 : Eu^{2+} , Dy^{3+} were evaluated in photocatalytic water decomposition for hydrogen production. The SrAl_2O_4 : Eu^{2+} , Dy^{3+} prepared by hydrothermal reaction exhibited excellent phosphor properties which were similar with that prepared by sol-gel method. Its photocatalytic activity for hydrogen evolution was higher than that of TiO_2 photocatalyst.

Keywords

Strontium Aluminate, Hydrothermal Reaction, Europium, Photocatalytic Activity, Sol-Gel Method, Water Spitting

1. Introduction

The alkaline earth aluminates have attracted a great attention as long afterglow materials because of their excellent photoluminescence, radiation intensity, color purity and good radiation resistance [1]. Especially, strontium aluminates co-doped with europium and dysprosium are used in the many fields due to its excellent phosphorescence. They are applied in an emergency lighting, safe indication, signposts, graphic arts, billboards, and interior design [2] [3] [4]. In addition, they can be introduced to synthesis new metal compound composite materials [5] and the cathode-ray tube and plasma display panel [6] [7]. They also present a photocatalytic activity as a photocatalyst due to their photosensitive properties [8].

The sol-gel process has drawn much interest to obtain novel chemical compositions and relatively lower reaction temperature resulting in homogeneous products [9]. It enables to synthesize the phosphors with small size. Recently, it has been concerned for the inorganic salt-based sol-gel approach rather than alkoxide-based sol-gel process in preparation of strontium aluminate luminescent materials [10] [11]. This is caused that the inorganic salts are usually nontoxic and cheaper than alkoxides.

Many methods for preparation of Eu^{2+} , Dy^{3+} -doped SrAl_2O_4 (SAO) had been studied such as a high temperature solid state reaction [12] [13], sol-gel method [14] [15] [16], co-precipitation method [17], combustion synthesis [18] [19], zone melting or laser melting [20] [21], microwave heating technique [22], and hydrothermal reaction method [23] [24]. Among these methods, the hydrothermal reaction is one of the most promising synthesis methods to obtain nanocrystallines having narrow particle size distribution, small particle size, crystallinity, good purity and well-controlled morphology. The method can be readily performed by a simple process with various starting materials at low temperatures without calcination [25]. The hydrothermal reaction method exhibits many advantages, such as a relatively low reaction temperature, high homogeneity and purity of the products. Therefore, nanosized phosphors that are uniformly distributed could be prepared by this method. In addition, it has suggested that the rare-earth fluoride nanocrystals can be changed gradually in growth with decreasing ionic radii by hydrothermal synthesis method [19]. However, the mixed reactants sol process should be calcined at higher temperature than 1000°C to prepare the SAO by sol-gel method. The calcination at lower temperature to the reactant sol is impossible to lead a good crystallinity of the SAO in the sol-gel method [26]. The calcining temperature should be lowered to accomplish a low-cost preparation in the synthesis process of SAO.

This report assessed the preparation of SAO by hydrothermal reaction through the process of calcination at lower temperature. The physical properties of the SAO were characterized in comparison with those of the SAO prepared by sol-gel method. The photocatalytic water decomposition using the SAO was performed to estimate its photocatalytic properties for hydrogen production.

2. Experimental

2.1. Preparation of SAOs

SAOs were prepared by both a sol-gel method and a hydrothermal reaction. In both methods, aluminum nitrate nonahydrate ($\text{Al}(\text{NO}_3)_3 \cdot 9\text{H}_2\text{O}$; 99.9%, Duksan), strontium nitrate ($\text{Sr}(\text{NO}_3)_2$; 99.9%, Duksan), dysprosium(III) nitrate pentahydrate ($\text{Dy}(\text{NO}_3)_3$; 99.9%, Alfa Aesar), and europium(III) nitrate hexahydrate ($\text{Eu}(\text{NO}_3)_3$; 99.9%, Alfa Aesar) were dissolved in distilled water with stirring for 30 min at 90°C . The solutions were conjugated according to the molar ratio of $\text{Sr}:\text{Al}:\text{Eu}:\text{Dy} = 0.97:2:0.01:0.02$. The entire reactant chemicals were analytical grade and used without further purification. All chemicals were kept in an au-

to-dry desiccator to prevent an admission of humidity.

The chelating reagent solution prepared by the appropriate amount of citric acid aqueous solution was added dropwise into the above solution. A boric acid solution was added into the solution with the chelating reagent solution. The mixture was concentrated at 80 °C with stirring until it changed a high viscosity translucent gel. Then, the mixture was calcined in a electric muffle furnace at 1100 °C for 3 h in a weak reducing atmosphere by hydrogen contained gas mixture (Ar:H₂ = 95:5).

SAO was also prepared by hydrothermal reaction. The mixture of SAO precursors and the chelating agent solution were poured into an autoclave. The autoclave contained the reactant was heated to 130 °C with stirring by magnetic stirrer. The hydrothermal reaction conditions were maintained for 5 h. The pressure of autoclave inside was retained ca. 3.8 kg/cm² during the hydrothermal synthesis. After the hydrothermal reaction, the product was dried at 110 °C for 12 h. Then, it was calcined at 550 °C for 4 h in the reducing atmosphere.

Commercially available TiO₂ (Degussa, P25) was employed as a control material in photocatalytic water decomposition. Ag ions were loaded on TiO₂ and SAO according to the method of typical incipient wetness impregnation. Silver(II) chloride (98%, Duksan) was used as a precursor of the Ag/TiO₂ and Ag/SAO photocatalysts. The Ag ions were incorporated on the photocatalyst crystallines at a 2 wt% the theoretical content.

2.2. Photocatalytic Decomposition of Water

The photocatalytic water decomposition was performed in an air-free closed gas circulation system which is connected to a GC with vacuum line. Distilled water was introduced as a reactant. Photocatalyst (1 g) was suspended with 400 ml of the water by magnetic stirring. A high pressure Hg lamp (Ace glass, 450 W) installed within the reactor was irradiated into the water. After air was excluded, Nitrogen gas was introduced by ca. 300 Torr before the irradiation. Gaseous products were quantitatively analyzed by GC (Shimadzu GC-10A).

2.3. Characterization of the SAOs

Phase identification of the SAOs particles was measured by X-ray diffraction (XRD) patterns, which was conducted on X-ray diffractometer (Rigaku Model D/max-II B). The XRD patterns was measured at 40 kV and 30 mA with a scan speed of 5°/min, scanning angle from 10° to 60°, and a step of 0.02° using Cu K α X-rays. Crystal size and morphologies of the SAOs were investigated by scanning electron microscopy (SEM; Hitachi S-4700). Their chemical components were analyzed by energy dispersive X-ray spectroscopy (EDS; NORAN Z-MAX 300 series). The N₂ isotherms of the SAO were investigated using the volumetric adsorption apparatus (Mirae SI, Porosity-X) at liquid N₂ temperature. The sample was pretreated at 150 °C for 1 h before exposure to nitrogen gas. Surface areas of samples were calculated by the BET equation [27]. Transmission electron mi-

croscopy (TEM; JEOL JEM-2100F) was measured using a LaB₆ filament and operated at 200 kV.

The compositions of phosphors were analyzed using an energy EDX micro analyzer (PGI IMIX PC) mounted on the microscope. The photoluminescent properties were evaluated with a photoluminescent spectrum (Hitachi F-4500). UV-vis diffuse reflectance spectra (DRS) were measured using a UV-vis spectrometer (Shimadzu UV-2450) in the region, 200 - 700 nm using BaSO₄ as the reflectance standard. The optical bandgap energy (E_{gap}) was calculated according to Kubelka and Munk method for the indirect electronic transitions.

3. Results and Discussion

3.1. Physicochemical Properties of the SAOs

Figure 1 shows the X-ray diffraction (XRD) patterns of the SAOs obtained by hydrothermal reaction and sol-gel method. It is defined that single-phase SAOs were obtained in the products prepared by the two methods. The positions and intensities of the main peaks of the two SAOs corresponded well with the standard card (No 34-0379). This indicates that the products preserved the pure SrAl₂O₄ phase. SEM images of SAOs synthesized by hydrothermal reaction and sol-gel method are shown in **Figure 2**. The morphologies and microstructure of the SAO powders can be observed from the SEM images. The SAOs were single-phase crystallites, and the particles were sintered into irregular shapes owing to the high calcination temperature.

Figure 3 presents energy dispersive X-ray spectra (EDS) of SAOs prepared by hydrothermal reaction and sol-gel method. The peaks of the Sr and Al elements exhibited in the SAOs. The intensity of SAO prepared by hydrothermal reaction

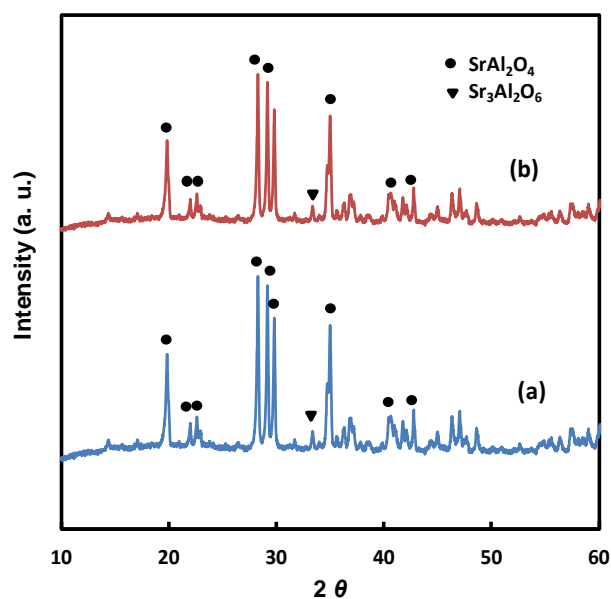


Figure 1. XRD patterns of SAOs synthesized by (a) hydrothermal reaction and (b) sol-gel method.

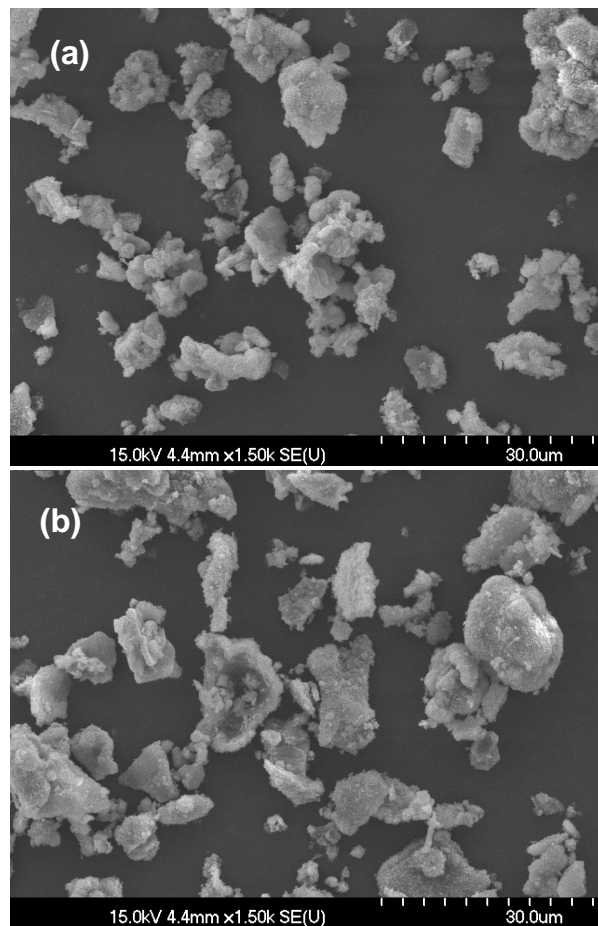


Figure 2. SEM images of SAOs synthesized by (a) hydrothermal reaction and (b) sol-gel method.

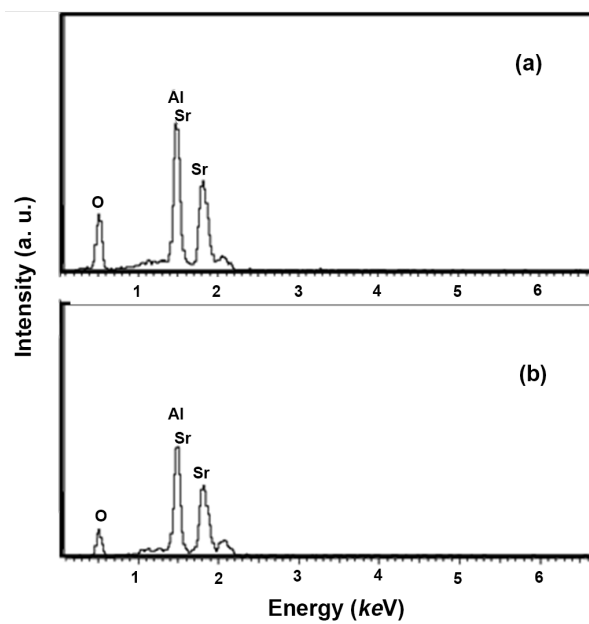


Figure 3. EDS of SAOs synthesized by (a) hydrothermal reaction and (b) sol-gel method.

was similar to that of prepared by sol-gel method. N_2 isotherm of SAO prepared by hydrothermal reaction is shown in **Figure 4**. The SAO is composed with single crystal as defined in SEM images. Type of isotherm of the SAO represents a typical adsorption pattern of nonporous particles. The hysteresis appeared in the isotherm curve is derived from some crevices between the particles. The specific surface area determined from BET equation was $62.5 \text{ m}^2/\text{g}$.

3.2. Luminescent Properties of the SAOs Products

Figure 5 presents emission spectra and UV-visDRS of the SAOs prepared by hydrothermal reaction and sol-gel method. The luminescence properties of the SAOs particles were measured on the solid state at room temperature. The SAOs particles prepared by the preparation methods exhibited the same emission peaks centered at around 510 nm under an excitation of 350 nm. It is associated with the typical $4f^65d^1 \rightarrow 4f^7$ transition of the Eu^{2+} ion in SrAl_2O_4 . This strongly affected on the nature of the Eu^{2+} surroundings, where the shielding function of the electrons in the inner shell made the mixed states of the 4f and 5d split by the crystal field [28]. The special emissions of Dy^{3+} and Eu^{3+} were not founded in the spectra. It was deduced that Eu^{3+} ions in the precursor are reduced effectively into Eu^{2+} in condition of a weak reducing atmosphere. Then, Eu^{2+} ions in the precursor are reduced effectively into Eu^+ , Dy^{3+} ions are oxidized into Dy^{4+} during the excitation [29]. Simultaneously, thermal vibrations of surrounding ions and local vibrations in the lattice structure are resulted in luminescence spectra with the broad bands [23]. The SAO prepared by hydrothermal reaction through a lower temperature calcination exhibited same emission intensity with the SAO prepared by sol-gel method through a high at temperature calcination.

Figure 5(b) presents UV-vis DRS results of the SAOs and TiO_2 converted as Kubelka-Munk units. The optical properties of the SAOs were induced by light

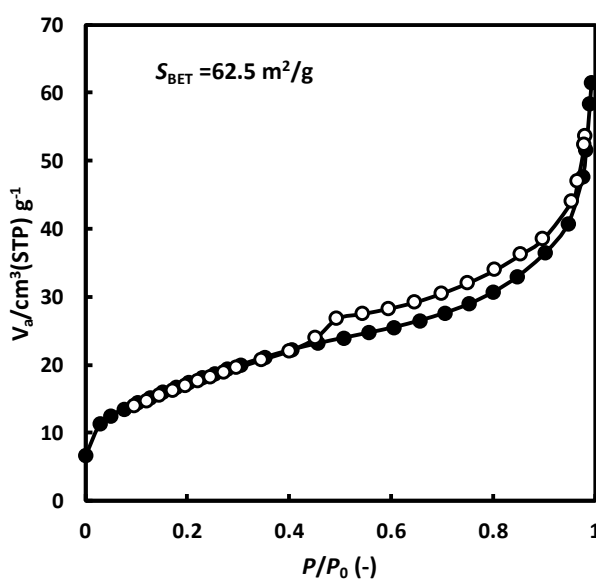


Figure 4. N_2 isotherm of SAO prepared by hydrothermal reaction.

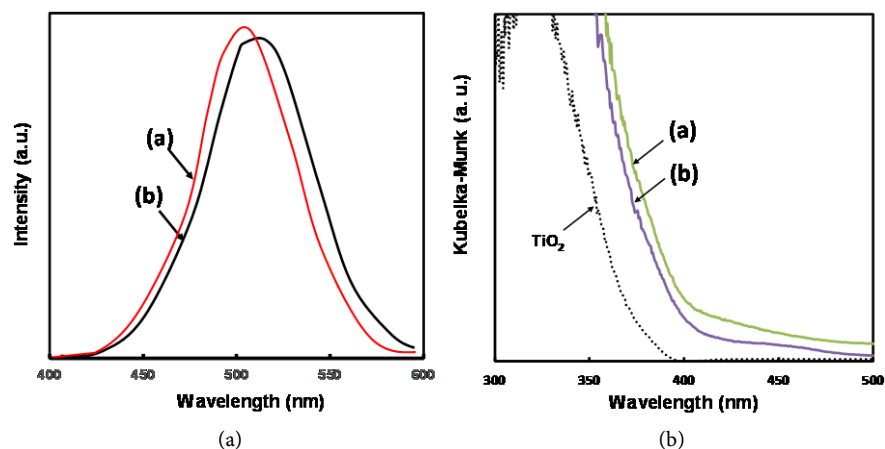


Figure 5. Emission spectra (a) and UV-vis DRS (b) of the SAOs prepared by (a) hydrothermal reaction and (b) sol-gel method.

absorption in the photochemical reaction. The diffuse reflectance spectrum of TiO_2 showed an adsorption edge at ca. 380 nm. The bandgap of TiO_2 determined from adsorption edge was 3.2 eV. Whereas, the DRS of SAOs were shifted the upper range of wavelength. The SAOs exhibited a significant increase of wavelength. The bandgap of the SAOs were ca. 2.9 eV.

3.3. Photocatalytic Properties of the SAOs

Hydrogen was generated in the gaseous products with a small amount of oxygen from water photocatalytic decomposition. No new liquid products were formed during the photocatalysis. The fundamental photocatalytic water splitting on photocatalyst involves multiple steps, including light absorption by the photocatalyst, photoexcitation of charge carriers (electron-hole pairs), separation of excited charges, migration of charge carriers to the photocatalyst surface, the transfer of charge carriers to water or other molecules, and surface reaction for H_2 or O_2 formation. **Figure 6** shows the rate of hydrogen evolution over TiO_2 and SAO prepared by hydrothermal reaction. Hydrogen was evolved by UV irradiation on the SAO phosphor. The rate on SAO was higher than that on TiO_2 photocatalyst. It seems that the higher photocatalytic activity of SAO was attributed to its higher photosensitivity, which has defined in the DRS results. The SAO represented a lower bandgap than TiO_2 . The hydrogen evolution rate was improved with Ag loading on the TiO_2 and SAO surface.

4. Conclusion

Eu^{2+} , Dy^{3+} -doped SrAl_2O_4 phosphor was prepared by a hydrothermal reaction through the lower temperature calcination. The physicochemical properties of the SrAl_2O_4 : Eu^{2+} , Dy^{3+} were characterized and compared to those of the SAO prepared by sol-gel method. The photocatalytic properties of the SAO were evaluated in photocatalytic water decomposition for hydrogen production. The SAO prepared by hydrothermal reaction presented similar properties of the SAO

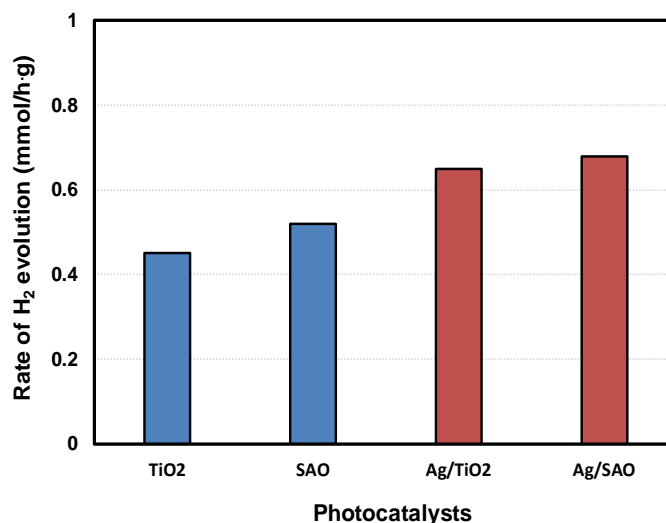


Figure 6. Rate of hydrogen evolution from water photocatalysis on various photocatalysts at 1 h of UV lamp irradiation.

phosphor prepared by sol-gel method. Though the SAO calcined at lower temperature, the characteristics of SAO matched well with the standard. Its photocatalytic activity for hydrogen evolution was higher than that of TiO₂ photocatalyst.

Acknowledgements

This paper was supported by Research Funds of Kwangju Women's University in 2017.

References

- [1] Du, H., Shan, W., Wang, L., Xu, D., Yin, H., Chen, Y. and Guo, D. (2016) Optimization and Complexing Agent-Assisted Synthesis of Green SrAl₂O₄: Eu²⁺, Dy³⁺ Phosphors through Sol-Gel Process. *Journal of Luminescence*, **176**, 272-277. <https://doi.org/10.1016/j.jlumin.2016.04.003>
- [2] Katsumata, T., Nabae, T., Sasajima, K. and Matsuzawa, T. (1998) Growth and Characteristics of Long Persistent SrAl₂O₄- and CaAl₂O₄-Based Phosphor Crystals by a Floating Zone Technique. *Journal of Crystal Growth*, **183**, 361-365. [https://doi.org/10.1016/S0022-0248\(97\)00308-4](https://doi.org/10.1016/S0022-0248(97)00308-4)
- [3] Nakamura, T., Kaiya, K., Takahashi, N., Matsuzawa, T., Rowlands, C.C., Beltran-Lopez, V., Smith, G.M. and Riedi, P.C. (2000) High Frequency EPR of Europium(II)-Doped Strontium Aluminate Phosphors. *Journal of Materials Chemistry*, **10**, 2566-2569. <https://doi.org/10.1039/b004061o>
- [4] Lin, Y., Tang, Z. and Zhang, Z. (2001) Preparation of Long-Afterglow Sr₄Al₁₄O₂₅-Based Luminescent Material and Its Optical Properties. *Materials Letters*, **51**, 14-18. [https://doi.org/10.1016/S0167-577X\(01\)00257-9](https://doi.org/10.1016/S0167-577X(01)00257-9)
- [5] Singh, T.S. and Mitra, S. (2007) Fluorescence Behavior of Intramolecular Charge Transfer State in *Trans*-Ethyl *p*-(Dimethylamino) Cinamate. *Journal of Luminescence*, **127**, 508-514. <https://doi.org/10.1016/j.jlumin.2007.03.001>
- [6] Kubota, S., Yamane, H. and Shimada, M. (2002) A New Luminescent Material,

- $\text{Sr}_3\text{Al}_{10}\text{SiO}_{20}:\text{Tb}^{3+}$. *Chemistry of Materials*, **14**, 4015-4016.
<https://doi.org/10.1021/cm025607o>
- [7] Lin, C.C., Xiao, Z.R., Guo, G.-Y., Chan, T.-S. and Liu, R.-S. (2010) Versatile Phosphate Phosphors ABPO_4 in White Light-Emitting Diodes: Collocated Characteristic Analysis and Theoretical Calculations. *Journal of the American Chemical Society*, **132**, 3020-3028. <https://doi.org/10.1021/ja9092456>
- [8] Kiss, B., Manning, T.D., Hesp, D., Didor, C., Taylor, A., Pickup, D.M., Chadwick, A.V., Allison, H.E., Dhanak, V.R., Claridge, J.B., Darwent, J.R. and Rosseinsky, M. (2017) Nano-Structured Radium Doped SrTiO_3 -Visible Light Activated Photocatalyst for Water Decomposition. *Applied Catalysis B: Environmental*, **200**, 547-555. <https://doi.org/10.1016/j.apcatb.2017.01.066>
- [9] Xiao, L.Y., Xiao, Q. and Liu, Y.L. (2011) Preparation and Characterization of Flower-Like $\text{SrAl}_2\text{O}_4:\text{Eu}^{2+}, \text{Dy}^{3+}$ Phosphors by Sol-Gel Process. *Journal of Rare Earths*, **29**, 39-43. [https://doi.org/10.1016/S1002-0721\(10\)60405-X](https://doi.org/10.1016/S1002-0721(10)60405-X)
- [10] Chai, Y.S., Zhang, P. and Zheng, Z.T. (2008) Eu^{2+} and Dy^{3+} Co-Doped $\text{Sr}_3\text{Al}_2\text{O}_6$ Red Long-Afterglow Phosphors with New Flower-Like Morphology. *Physica B: Condensed Matter*, **403**, 4120-4122. <https://doi.org/10.1016/j.physb.2008.08.011>
- [11] Suriyamurthy, N. and Panigrahi, B.S. (2008) Effects of Non-Stoichiometry and Substitution on Photoluminescence and Afterglow Luminescence of $\text{Sr}_4\text{Al}_{14}\text{O}_{25}:\text{Eu}^{2+}, \text{Dy}^{3+}$ Phosphor. *Journal of Luminescence*, **128**, 1809-1814. <https://doi.org/10.1016/j.jlumin.2008.05.001>
- [12] He, Z., Wang, X. and Yen, W.M. (2006) Investigation on Charging Processes and Phosphorescent Efficiency of $\text{SrAl}_2\text{O}_4:\text{Eu}, \text{Dy}$. *Journal of Luminescence*, **119-120**, 309-313. <https://doi.org/10.1016/j.jlumin.2006.01.010>
- [13] Ayari, M., Paul-Boncour, V., Lamloumi, J., Mathlouthi, H. and Percheron-Guégan, A. (2006) Study of the Structural, Thermodynamic and Electrochemical Properties of $\text{LaNi}_{3.55}\text{Mn}_{0.4}\text{Al}_{0.3}(\text{Co}_{1-x}\text{Fe}_x)_{0.75}$ ($0 \leq x \leq 1$) Compounds Used as Negative Electrode in Ni-MH Batteries. *Journal of Alloys and Compounds*, **420**, 251-255. <https://doi.org/10.1016/j.jallcom.2005.10.034>
- [14] Peng, T., Huajun, L., Yang, H. and Yan, C. (2004) Synthesis of $\text{SrAl}_2\text{O}_4:\text{Eu}, \text{Dy}$ Phosphor Nanometer Powders by Sol-Gel Processes and Its Optical Properties. *Materials Chemistry and Physics*, **85**, 68-72. <https://doi.org/10.1016/j.matchemphys.2003.12.001>
- [15] Cordoncillo, E., Julian-Lopez, B., Martínez, M., Sanjuán, M.L. and Escribano, P. (2009) New Insights in the Structure-Luminescence Relationship of $\text{Eu}:\text{SrAl}_2\text{O}_4$. *Journal of Alloys and Compounds*, **484**, 693-697. <https://doi.org/10.1016/j.jallcom.2009.05.018>
- [16] Rezende, M.V., Montes, P.J., Soares, F.M., Santos, C. and Valerio, M.E. (2014) Influence of Co-Dopant in the Europium Reduction in SrAl_2O_4 Host. *Journal of Synchrotron Radiation*, **21**, 143-148. <https://doi.org/10.1107/S1600577513025708>
- [17] Tao, J., Pan, H., Zhai, H., Wang, J., Li, L., Wu, J., Jiang, W., Xu, X. and Tang, R. (2009) Controls of Tricalcium Phosphate Single-Crystal Formation from Its Amorphous Precursor by Interfacial Energy. *Crystal Growth & Design*, **9**, 3154-3160. <https://doi.org/10.1021/cg801130w>
- [18] Zhang, R., Han, G., Zhang, L. and Yan, B. (2009) Gel Combustion Synthesis and Luminescence Properties of Nanoparticles of Monoclinic $\text{SrAl}_2\text{O}_4:\text{Eu}^{2+}, \text{Dy}^{3+}$. *Materials Chemistry and Physics*, **113**, 255-259. <https://doi.org/10.1016/j.matchemphys.2008.07.084>
- [19] Peng, T., Yang, H., Pu, X., Hu, B., Jiang, Z. and Yan, C. (2004) Combustion Synthe-

- sis and Photoluminescence of SrAl₂O₄: Eu, Dy Phosphor Nanoparticles. *Materials Letters*, **58**, 352-356. [https://doi.org/10.1016/S0167-577X\(03\)00499-3](https://doi.org/10.1016/S0167-577X(03)00499-3)
- [20] Katsumata, T., Sakai, R., Komuro, S., Morikawa, T. and Kimura, H. (1999) Growth and Characteristics of Long Duration Phosphor Crystals. *Journal of Crystal Growth*, **198**, 869-871. [https://doi.org/10.1016/S0022-0248\(98\)01132-4](https://doi.org/10.1016/S0022-0248(98)01132-4)
- [21] Aroz, R., Lennikov, V., Cases, R., *et al.* (2012) Laser Synthesis and Luminescence Properties of SrAl₂O₄: Eu²⁺, Dy³⁺ Phosphors. *Journal of the European Ceramic Society*, **32**, 4363-4369. <https://doi.org/10.1016/j.jeurceramsoc.2012.06.013>
- [22] Wu, S.L., Zhang, S.F. and Yang, J.Z. (2007) Influence of Microwave Process on Photoluminescence of Europium-Doped Strontium Aluminate Phosphor Prepared by a Novel Sol-Gel Microwave Process. *Materials Chemistry and Physics*, **102**, 80-87. <https://doi.org/10.1016/j.matchemphys.2006.11.003>
- [23] Xiao, Q., Xiao, L., Liu, Y., Chen, X. and Li, Y. (2010) Synthesis and Luminescence Properties of Needle-Like SrAl₂O₄: Eu, Dy Phosphor via a Hydrothermal Co-Precipitation Method. *Journal of Physics and Chemistry of Solids*, **71**, 1026-1030. <https://doi.org/10.1016/j.jpics.2010.04.017>
- [24] Wang, X., Zhuang, J., Peng, Q. and Li, Y. (2006) Hydrothermal Synthesis of Rare-Earth Fluoride Nanocrystals. *Inorganic Chemistry*, **45**, 6661-6665. <https://doi.org/10.1021/ic051683s>
- [25] Zhang, Y., Zhong, L. and Duan, D. (2015) Single-Step Hydrothermal Synthesis of Strontium Titanate Nanoparticles from Crystalline Anatase Titanium Dioxide. *Ceramics International*, **41**, 13516-13524. <https://doi.org/10.1016/j.ceramint.2015.07.145>
- [26] Liu, Y. and Xu, C.-N. (2003) Influence of Calcining Temperature on Photoluminescence and Triboluminescence of Europium-Doped Strontium Aluminate Particles Prepared by Sol-Gel Process. *Journal of Physical Chemistry B*, **107**, 3991-3995. <https://doi.org/10.1021/jp022062c>
- [27] Brunauer, S., Emmett, P.H. and Teller, E. (1938) Adsorption of Gases in Multimolecular Layers. *Journal of the American Chemical Society*, **60**, 309-319. <https://doi.org/10.1021/ja01269a023>
- [28] Shan, W., Wu, L., Tao, N., Chen, Y. and Guo, D. (2015) Optimization Method for Green SrAl₂O₄: Eu²⁺, Dy³⁺ Phosphors Synthesized via Co-Precipitation Route Assisted by Microwave Irradiation using Orthogonal Experimental Design. *Ceramics International*, **41**, 15034-15040. <https://doi.org/10.1016/j.ceramint.2015.08.050>
- [29] Hong, G.Y., Jeon, B.S., Yoo, Y.K. and Yoo, J.S. (2001) Photoluminescence Characteristics of Spherical Y₂O₃: Eu Phosphors by Aerosol Pyrolysis. *Journal of The Electrochemical Society*, **148**, H161-H166. <https://doi.org/10.1149/1.1406496>